SSRG International Journal of Civil Engineering
ISSN: 2348-8352/ https://doi.org/10.14445/23488352/IJCE-V13I7P101

Volume 13 Issue 7, 1-14, July 2026

Original Article

Tomographic Terahertz (THz) Wave Based Image Reconstruction for Subsurface Crack Identification in Civil Infrastructure Buildings

Surajit Mohanty[1], Subhendu Kumar Pani[2], Suvendu Tripathy[3], Achyutananda Rout[4], Rajeev Agarwal[5], Sunita Dalei[6]

[1]Computer Science and Engineering, Biju Patnaik University of Technology, Rourkela, Odisha, India.
[2]Computer Science and Engineering, Krupajal Computer Academy, Biju Patnaik University of Technology, Rourkela, Odisha, India.
[3,4,5]Computer Science and Engineering, School of Engineering and Technology, DRIEMS University, Tangi, Cuttack, Odisha, India.
[6]Department of CSE, Raajdhani Engineering College, Mancheswar, Bhubaneswar, Odisha, India.

[1]Corresponding Author : bivaan2024@gmail.com

Received: 19 March 2026 Revised: 01 June 2026 Accepted: 19 June 2026 Published: 29 July 2026

Abstract - *Detection of cracks in civil infrastructure buildings at an early age is very much important to give these structures structural safety, serviceability and long life. Traditional Non-Destructive Testing (NDT) methods, which include visual inspection, ultrasonic testing and infrared thermography, are usually limited to detect concealed or near-surface defects especially on heterogeneous building materials. This paper introduces a Terahertz (THz) wave-based imaging technology to be able to detect and identify subsurface cracks in civil infrastructure buildings non-invasively. Thanks to the capacity of poring non-metallic materials, including concrete, masonry, and composites, THz imaging allows detecting internal discontinuities of high resolution without being in physical contact or preparing the surface. The suggested framework combines THz time-domain imaging and improved signal processing and image reconstruction algorithms to improve the visibility of cracks and depth discrimination. The test studies done on model building materials show that the THz system has the potential to identify the existence of both micro- and macro-level under-surface cracks which cannot be detected by other conventional methods. The findings suggest that THz wave based imaging has a high potential as an intelligent, non-destructive assessment instrument of early damage and structural health monitoring of civil infrastructure buildings.*

Keywords - *Terahertz imaging, Civil infrastructure buildings, Structural Health Monitoring, Subsurface crack detection, Terahertz time-domain spectroscopy, Non-Destructive Testing.*

1. Introduction

The issue of structural integrity and durability of civil infrastructure buildings is becoming more and more challenging due to aging, exposure to the environment, and an increase in service needs, and the early identification of internal damage is an essential factor contributing to successful maintenance and risk prevention. Subsurface cracks are a major deterioration factor among others because most of the time, they can go unnoticed until they extend to the surface of the ground or result in serious structural damages. Traditional Non-Destructive Tests (NDT) methods, like visual inspection, ultrasonic tests, ground penetrating radar and infrared thermography, have limitations to detect reliably the shallow or hidden cracks in heterogeneous construction materials, including concrete and masonry. Terahertz (THz) wave-based imaging has become a potential solution to subsurface damage in this scenario because it is non-ionizing, high-spatial resolution, and has a high sensitivity to material discontinuities. The majority of non-metallic building materials are penetrated by THz waves and in time-domain analysis the depth-resolved information allows the detection of internal defects without any physical contact and preparation of the surfaces. The recent developments in the source and detector of THz and signal processing strategies have increased the imaging capability and practical feasibility. Therefore, the THz imaging provides an innovative and smart method of non-invasive subsurface crack detection, which can be used to proactively monitor the structural health of a civil infrastructure building and detect its lifecycle more efficiently. According to Kwak et al., (2024), sub-terahertz imaging showed the ability to measure internal defect depth in real time and, therefore, the use of THz waves was confirmed as an effective method of subsurface inspection [1]. Deng and Liu (2011) defined the theoretical basis of electromagnetic imaging in NDT, which is the high quality resolution of high frequencies like terahertz of detecting hidden defects [2]. Yang et al., (2023) demonstrated that terahertz imaging, when paired with Faster R-CNN, has a substantial ability to enhance automated detection of defects in composite materials, which suggests that terahertz imaging can be utilized to perform intelligent crack detection [3]. Kumpati et al., (2021) revised the integrated NDT methods and found THz imaging as one of the newer methods in this category, which has the potential to surpass the shortcomings of more traditional methods [4]. Kruegener et al., (2020) managed to use THz inspection on buildings and architectural heritage and prove the efficiency of the method in identifying subsurface cracks in masonry and concrete without contact [5]. Civera and Surace (2022) also mentioned that the techniques of NDT were advanced in terms of structural health monitoring, noting that non-invasive and high-resolution methods were required [6]. Yue et al., (2024) suggested single-shot broadband THz imaging, which is much faster and can be applied in practice in large volumes during inspections [7]. The studies by Alaggio et al., (2021) and Aloisio et al., (2021) have shown that long-term static, dynamic, and seismic monitoring give important information on structural degradation of heritage buildings [8, 9], and Clementi et al., (2021) have highlighted the development of SHM toward intelligent, data-driven systems [10]. The damage in concrete structures, caused by corrosion, was examined by Di Benedetto et al., (2021) and Rosso et al., (2022), which makes it essential to detect the damage at the subsurface level at its initial stages [11, 12].

Rosso et al., (2022) conducted a literature review of the implementation of deep learning in SHM and validated the increasingly significant role of AI in the identification of damage [13]. The study by Parisi et al., (2022), Sony et al., (2022), and Flah et al., (2022) showed that machine learning and deep learning are effective in localizing and classifying damages through vibration [14-16]. Deep learning-based vision-based crack detection was confirmed by Yu et al., (2022a, 2022b), but these modalities can only be used to detect defects on the surface [17, 18]. The scalability of high-throughput image analysis was demonstrated by Guo et al., (2022) [19], which was further developed by Rosso et al., (2023) and Rosso et al., (2023) to intelligent monitoring based on analytical models, convolutional networks, and transformers [20, 21].

Lastly, Mesaros et al., (2021) noted the advanced signal interpretation methods applicable to multi-sensor SHM systems [22]. Taken together, these studies indicate that there is an evident gap in research in terms of incorporating the concept of terahertz wave-based imaging with intelligent analytics to deliver reliable subsurface crack detection in civil infrastructure structures. The general results of the literature review show that the traditional non-destructive methods of testing and the AI-assisted vision or vibration techniques are efficient to detect the surface-based or global-based damages but fail to detect the early subsurface cracks in heterogeneous construction materials. The Terahertz (THz) based imaging is an attractive solution because it is a non-contact imaging technique, which has high spatial resolution and penetrates non-metallic civil infrastructure materials. The solution process incorporates THz time-domain imaging, superior signal processing and smart data-driven algorithms to boost the visibility of cracks, depth estimation and reliability, so that proactive structural health can be done in early stages of crack detection and proactively prevent the complex process of maintenance and structures.

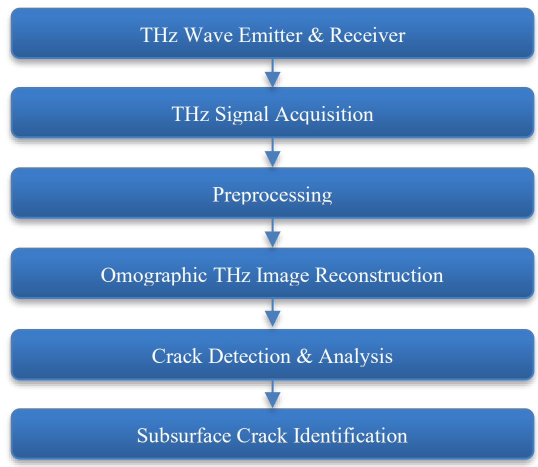

Fig. 1 Proposed framework of intelligent workflow for subsurface crack identification in civil infrastructure buildings

In Figure 1, the proposed framework presents a sophisticated and smart workflow of identifying subsurface cracks in civil infrastructure buildings with Terahertz (THz) wave-based imaging. This happens by starting with the THz wave emitter and receiver and transmitting short pulses in the THz at the emitter and receiver into non-metallic building materials and collecting the reflected signals of internal discontinuities. The aquiring of these reflected responses is in the form of time-domain data, which is what the subsurface analysis is based on. The data is then subjected to preprocessing and signal enhancement to remove noise, equalize signal levels and remove undesired artifact to enhance data quality. The high signal processing methods such as time analysis, depth mapping, and 3D image reconstruction are then used to view the internal structural characteristics and where possible crack areas can be found. Intelligent analysis block combines both machine learning and artificial intelligence algorithms to automatically identify the meaningful features and differentiate the presence of cracks and the heterogeneity of the material. The crack identification and outcomes phase offers reliable localization of underground cracks and depth estimation and damage determination. Damage quantification also measures crack length, width and severity of the damage which makes it possible to objectively evaluate the condition. Lastly, the framework enables temporal tracking via repetitive THz scanning and time series analysis to track the propagation of cracks, report on the condition, and provide maintenance alerts as a part of an overall structural health monitoring and reporting system [23].

Accurate, timely identification of defects, especially those located at the substructure level, in concrete, masonry, and composite materials is crucial for the safety, durability and serviceability of civil infrastructure buildings. Most of these hidden flaws are not discovered until the structures are significantly damaged, causing expensive maintenance costs, poor structural performance and safety hazards. Visual inspection, ultrasonic testing, Ground-Penetrating Radar (GPR), infrared thermography and X-ray computed tomography (X-ray CT) are some of the conventional Non-Destructive Evaluation (NDE) techniques commonly used to assess cracks. These methods, however, often have a number of drawbacks, including poor spatial resolution, low sensitivity to defects at shallow depths, high operating expense, safety concerns, or requirement of material properties and environmental conditions.

Terahertz (THz) imaging is a recently developed technology with great promise that enables non-contact, non-ionizing and high-resolution subsurface inspection. However, current research is mainly concerned with material characterization and/or defect detection on a laboratory scale, and few studies have investigated tomographic image reconstruction of THz signals for accurate localization and quantitative assessment of crack defects for civil infrastructure applications. Moreover, there is still a lack of research on advanced signal processing and intelligent damage characterization for SHM (SHM). This study aims to fill these research gaps by proposing a Tomographic Terahertz (THz) Wave Based Image Reconstruction framework for subsurface crack identification in civil infrastructure buildings. This novelty is based on the use of THz time-domain imaging, reconstruction through tomography, depth-resolved analysis and intelligent crack quantification for the accurate detection, localization and characterization of hidden defects. The developed framework offers high-resolution imaging, high-sensitivity crack detection and structural condition assessment, enabling proactive maintenance and next-generation structural health monitoring systems.

2. Methodology

2.1. Terahertz Data Acquisition System

The proposed methodology employs a Terahertz Time-Domain Imaging (THz-TDI) system comprising a broadband THz wave emitter and a sensitive receiver operating in reflection mode. Short-duration THz pulses are transmitted into non-metallic civil infrastructure materials such as concrete and masonry. Subsurface cracks, voids, and material discontinuities cause variations in dielectric properties, resulting in partial reflection and scattering of the incident THz waves. The reflected signals are captured at multiple spatial locations through raster scanning to generate two-dimensional and three-dimensional datasets. This non-contact and non-ionizing acquisition process ensures safe and rapid inspection without requiring surface preparation or structural disruption.

THz Back-Scattered Field Model:

$$E_r(r,t) = \iiint_{\Omega}^{t} E_i\left(t - \frac{2|r-r'|}{v\varepsilon_r}\right)\Gamma(r')exp(-\alpha \mid r - r' \mid)dr' + n(t) \quad (1)$$

Frequency-Domain Reflection Coefficient due to Crack Interface:

$$\Gamma(f,r) = \frac{\sqrt{\varepsilon_h(f)}-\sqrt{\varepsilon_c(f,r)}}{\sqrt{\varepsilon_h(f)}+\sqrt{\varepsilon_c(f,r)}} \exp\left(-j\frac{4\pi f}{c} d(r)\sqrt{\varepsilon_c(f,r)}\right) \quad (2)$$

Crack Depth Estimation Using Time-of-Flight (ToF):

$$d(r) = \frac{c}{2}\frac{\Delta t(r)}{\sqrt{\varepsilon_r(f)}} \quad (3)$$

Tomographic THz Image Reconstruction with Regularization:

$$\varepsilon\hat{} = \underset{\varepsilon}{arg}\, min \parallel Er - F(\varepsilon,r,t) \parallel_2^2 + \lambda \int_{\Omega}^{r} \parallel \nabla\varepsilon(r) \parallel_1 dr \quad (4)$$

Crack Severity Index from Multi-Parametric THz Features:

$$C_{THz} = \sum_{i=1}^{N} w_i\left[\frac{\Delta t_i}{t_0} + \frac{\Delta A_i}{A_0} + \frac{\Delta\varepsilon_i}{\varepsilon_0}\right] \quad (5)$$

Equations (1) to (5) together establish a comprehensive THz-based framework for subsurface crack detection and characterization in civil infrastructure. Equation (1) models the received back-scattered THz signal as a cumulative response from all subsurface scatterers, incorporating propagation delay, dielectric-dependent velocity, attenuation, reflection strength, and measurement noise, thereby capturing how internal cracks influence the measured echo. Equation (2) describes the frequency-domain reflection coefficient at the crack interface, where dielectric contrast between the host material and crack region governs amplitude and phase variations, enabling depth-dependent crack identification. Equation (3) uses the time-of-flight principle to estimate crack depth by converting the measured round-trip delay into physical distance using the effective permittivity. Equation (4) formulates tomographic image reconstruction as a regularized inverse problem, balancing data fidelity with edge-preserving constraints to enhance crack boundaries in reconstructed permittivity maps. Finally, Equation (5) integrates multi-parametric THz features, including delay, amplitude loss, and permittivity variation, into a unified crack severity index, allowing quantitative assessment of damage extent and intensity.

Full electrodynamic plate equation with distributed actuation source term:

$$\rho \frac{\partial^2 u(r,t)}{\partial t^2} = \nabla \cdot \left(C(r) \colon \nabla^s u(r,t) \right) + f_{UGH}(r,t) + f_{AE}(r,t), \quad (6)$$

$$f_{UGH}(r,t) = \sum_{i=1}^{N_{PZT}} a_i(t) \delta(r - s_i), \quad f_{AE}(r,t) = \sum_{j=1}^{N_{AE}} b_i(t) \delta(r - q_j), \quad (7)$$

(ρ mass density; $C(r)$ stiffness tensor; ∇s symmetric gradient; *PZT* actuators at s_i and AE point sources at q_j).

Rayleigh–Lamb dispersion transcendental equations (symmetric & antisymmetric modes):

$$\begin{cases} tan(qh)tan(ph) = -\frac{4k^2pq}{(k^2-q^2)^2} \quad (symmetric\ modes) \\ tan(qh)tan(ph) = -\frac{(k^2-q^2)^2}{4k^2pq} \quad (antisymmetric\ modes) \end{cases} \quad (8)$$

with $$p^2 = \frac{\omega^2}{C_L^2} - k^2; \quad q^2 = \frac{\omega^2}{C_T^2} - k^2; k = \frac{\omega}{c_p} \quad (9)$$

(h half-thickness, C_L^2 longitudinal and shear wave speeds. Use to compute $c_p(\omega)$ and modal structure for signal propagation.)

Scattering perturbation (Born approximation) for a small stiffness perturbation ΔC:

$$\delta u(r,\omega) \approx \omega^2 \int_{\Omega_d} G(r, r'; \omega) \colon \Delta C(r') \colon u_0(r', \omega) dr', \quad (10)$$

(G elastodynamic Green's tensor; u_0 incident (unperturbed) field; integral gives first-order scattered field from crack/damage domain Ω_d.)

2.2. Signal Preprocessing and Feature Enhancement

Raw THz signals are often affected by noise, surface roughness effects, and material heterogeneity. To address these challenges, preprocessing techniques such as background subtraction, temporal windowing, normalization, and band-pass filtering are applied. These steps enhance signal-to-noise ratio and suppress unwanted reflections from surface layers. Time-domain features, including peak amplitude, time delay, and pulse width variations, are extracted to highlight subsurface anomalies. Enhanced signals form a reliable basis for further depth estimation and crack characterization. The two sensing modalities can be combined whereby it would facilitate data fusion that improves the accuracy of crack localization based on Time of Flight (TOF) and Time Difference of Arrival (TDOA) responses. Advanced signal processing plans such as cross correlation, likelihood ratio detect- boost Signal to Noise Ratio (SNR) and reduce false alarms. The two combined will ensure timely, precise and reliable structural anomalies that would increase the lifespan of the buildings, enhance the maintenance plan and significantly reduce disastrous collapses along the civil infrastructure systems.

False alarm / detection probabilities (Gaussian approx.):

$$P_{FA} = Q\left(\frac{\gamma-\mu_0}{\sigma_0}\right), P_{DA} = Q\left(\frac{\gamma-\mu_1}{\sigma_1}\right) \quad (11)$$

(Q tail function; μ, σ under hypotheses.)
Sensor spacing constraint to meet spatial Nyquist for wavelength λ:

$$d_{max} \leq \frac{\lambda_{min}}{2} = \frac{c_{min}}{2f_{max}} \quad (12)$$

(Inter-sensor distance *d* is taken to avoid aliasing of wavefield spatially.)

Coverage probability with sensors (Poisson approx.):

$$P_{conv}(x) = 1 - \prod_{i=1}^{N} (1 - 1\{\parallel x - s_i \parallel \leq R_i\}) \quad (13)$$

(Indicator if point *x* is within any sensor effective radius R_i.)

CRLB (Cramér–Rao Lower Bound) for 2D TDOA (Time Difference of Arrival) localization variance (approx.):

$$Var(x^\wedge) \geq J^{-1}, J = \sum_i \frac{1}{\sigma_{t,i}^2} \nabla_x \tau_i \nabla_x \tau_i^\top \quad (14)$$

(J Fisher information, $\sigma_{t,i}^2$ timing jitter.)

Optimization objective for sensor placement (maximize info / minimize error):

$$min_{\{s_i\}}\ trace\ (J^{-1}(\{s_i\}));\ s.t. s_i \in A \quad (15)$$

(Design sensors s_i in area *A* to minimize localization variance.)

Coupling efficiency between Lead Zirconate Titanate (PZT) and structure (mechanical impedance match):

$$\eta_c = \frac{4Z_P Z_S}{(Z_P + Z_S)^2}, Z = \rho c A \quad (16)$$

($Z_P Z_S$ mechanical impedances of patch and substrate; *A* area.)

Modal conversion (mode scattering coefficient at defect):

$$S_{m\to n}(\omega) = \int_{\Omega_d} \Delta C(r) \Phi_m(r,\omega) \Phi_n^*(r,\omega) dr \quad (17)$$

(ΔC stiffness perturbation at defect domain Ω_d mode shapes.)

Depth-resolved information is obtained by analyzing the time-of-flight of reflected THz pulses, allowing accurate estimation of crack depth and internal geometry. Advanced signal processing techniques, including wavelet transforms and frequency-domain analysis, are employed to isolate crack-related responses from background material effects.

Three-dimensional image reconstruction algorithms convert processed signals into volumetric representations of the inspected region, enabling visualization of crack morphology, orientation, and spatial distribution within the structure.

2.3. Intelligent Crack Detection and Damage Assessment

Machine learning and artificial intelligence algorithms are integrated to automate crack detection and classification. Extracted features and reconstructed images are input to supervised or semi-supervised learning models to distinguish cracks from benign material variations. The intelligent framework quantifies crack parameters such as length, width, depth, and severity, supporting objective damage assessment. Repeated inspections enable temporal analysis for monitoring crack propagation and structural deterioration, facilitating proactive maintenance decisions and long-term structural health monitoring of civil infrastructure buildings. Matched-filter / correlation detector (maximizes SNR for known template):

$$y(t) = \int_{-\infty}^{\infty} S^*(\tau)x(t+\tau)d\tau \quad (18)$$

(Peak of $y(t)$ indicates best match of received signal x to template s.)

Magnitude-squared coherence between sensors i and j:

$$\gamma_{ij}^2(\omega) = \frac{|S_{ij}(\omega)|^2}{S_{ii}(\omega)S_{jj}(\omega)} \quad (19)$$

(Measures linear correlation at frequency ω; high values indicate common source/wave path.)

Delay-and-sum beamformer output (steering to direction / location):

$$\mathrm{y(t)} = \sum_{i=1}^{N} \omega_i x_i(t-\tau_i(p)) \quad (20)$$

(ω_i weights, $\tau_i(p)$ delays for focus point p; improves SNR/localization.)

Low-rank modal decomposition (SVD) of recorded wavefield matrix X):

$$X = U\Sigma V^{T}, X \in R^{M\times T} \quad (21)$$

(Columns = time snapshots; keep leading singular vectors for coherent mode extraction / noise suppression.)

Bayesian update for damage state θ:

$$p(\theta\,|y) \propto p(y\,|\theta)\,p(\theta) \quad (22)$$

(Posterior probability of damage parameters θ given measurements y; enables probabilistic localization/uncertainty.)

AUC (Area Under the Curve (Receiver Operating Characteristic)) as integral of TPR (True Positive Rate) over FPR (False Positive Rate) for crack determination:

$$\mathrm{AUC} = \int_0^1 TPR(FPR^\wedge - 1(\alpha))d\alpha \quad (23)$$

(Scalar measure of detector discrimination power; 1 = perfect, 0.5 = random.)

Sparse sensor selection via convex surrogate (ℓ1 relaxation):

$$\begin{cases} min \\ \omega \in [0.1] \end{cases} \lambda \parallel \omega \parallel_1 + trace\,(J^{-1}(\omega)) \quad (24)$$

(with $J(\omega)$Fisher information depending on active-sensor mask ω); (Trade-off between number of sensors (sparsity) and localization performance tune λ.)

The zones of coverage are stipulated according to the structural vulnerability and paths of waves. The densest distribution of sensors is made in critical areas that have greater stress gradients like load-transfer areas and reinforcement anchor areas. Epoxy adhesives or couplants such as silicone grease are to be used to couple the sensors and the surface to have a consistent acoustic impedance. In the case of concrete or composite materials, it is necessary to protect the sensors against environmental degradation and transmit the signals with the same quality, which is achieved through the use of waveguides or embedded patches of PZT. A dedicated framework for Structural Health Monitoring (SHM) integration is included to showcase the potential of using the proposed methodology for ongoing condition monitoring of civil structures. The SHM system integrates periodic sensing, automatic data acquisition, signal processing, defect detection and predictive maintenance in a single system that monitors the entire process.

Figure 2 illustrates the stepwise algorithm for THz-based subsurface crack detection using a reflection-mode raster scanning approach. The process begins with the initialization of the THz emitter and receiver, followed by configuring reflection-mode parameters and positioning the devices over the target area. A raster scan grid is established to systematically cover the surface, where short-duration THz pulses are transmitted at each position. The back-scattered signals are pre-processed and filtered to remove noise, and time-of-flight analysis extracts depth information of subsurface cracks. The data are stored, scan positions are incremented, and the loop repeats until all areas are scanned, completing data acquisition for subsequent tomographic reconstruction.

An inter-comparison study was carried out between the proposed Terahertz (THz) imaging approach and traditional Non-Destructive Evaluation (NDE) methods such as Ground Penetrating Radar (GPR), Ultrasonic Testing (UT), X-ray Computed Tomography (CT) and Infrared Thermography (IRT). Factors that were taken into consideration were key performance indicators like penetration depth, spatial resolution, crack sensitivity, operational safety, deployment complexity and inspection cost. The results show that THz imaging may be more effective in terms of spatial resolution and sensitivity for detecting shallow subsurface cracks in non-metallic civil infrastructure materials. THz imaging also is non-ionizing and safer for field use compared to X-ray CT, and it does not necessitate surface preparations as is the case for ultrasonic methods. The defects localization and depth characterization capabilities of THz imaging are better than those of GPR and infrared thermography, making it a potential option for high resolution structural health monitoring applications.

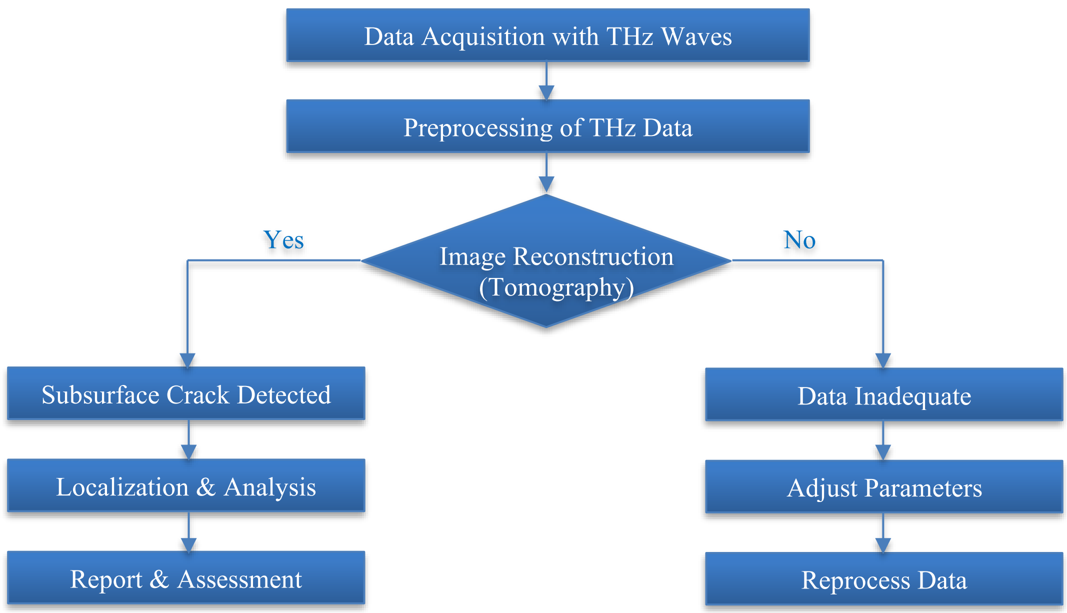

Fig. 2 Stepwise algorithm for THz-based subsurface crack detection

3. Experimental Setup and Data Analysis

The experimental setup for Tomographic Terahertz (THz) wave-based image reconstruction consists of a broadband pulsed THz Time-Domain Spectroscopy (THz-TDS) system integrated with a raster-scanning and rotational tomography platform. A femtosecond laser excites a photoconductive antenna to generate sub-picosecond THz pulses, which are directed toward reinforced concrete and masonry specimens containing artificial subsurface cracks of varying depths and orientations. The samples are mounted on a precision motorized stage that enables linear scanning and angular rotation, allowing the acquisition of multiple projection views essential for tomographic reconstruction. Both reflection-mode and transmission-mode measurements are performed depending on specimen thickness, with the reflected THz signals captured by a synchronized detector antenna. The recorded time-domain waveforms are pre-processed through baseline correction, noise filtering, and time-gating to isolate reflections from subsurface interfaces. Data analysis involves converting time-of-flight information into depth profiles using known dielectric properties of construction materials, followed by reconstruction using filtered back-projection and algebraic reconstruction techniques. Variations in signal amplitude, phase delay, and spectral attenuation are analyzed to distinguish crack-induced discontinuities from material heterogeneity. The reconstructed tomographic slices provide high-contrast visualization of crack geometry, depth, and extent, demonstrating the effectiveness of THz imaging as a non-destructive evaluation tool for civil infrastructure health monitoring. The test specimens comprise Reinforced Cement Concrete (RCC) blocks representative of building elements such as slabs and beams, cast using Ordinary Portland Cement (OPC, Grade 43), river sand, and crushed granite aggregate (maximum size 20 mm) with a mix proportion of 1:1.5:3 and a water–cement ratio of 0.45, achieving a compressive strength of 30–35 MPa after 28 days of curing. Specimens of size 300 mm × 300 mm × 100 mm are prepared with artificial subsurface cracks introduced during casting using non-metallic polyethylene or Teflon spacers of 0.3–3.0 mm thickness, positioned at depths of 5–60 mm and lengths of 20–120 mm, simulating both air-filled and moisture-filled crack conditions. The electromagnetic properties considered include a relative permittivity of 6.0–7.5 for intact dry concrete, approximately 1.0 for air-filled cracks, and 3.0–4.0 for moisture-filled cracks within the 0.3–1.5 THz band, with an effective electrical conductivity of about 0.01 S/m and attenuation coefficient of 3–5 cm^{-1}. To reduce surface scattering, specimens are finished to a surface roughness of ≤0.5 mm, with no exposed metallic reinforcement in the scanning zone, and selected samples are coated with a thin dielectric epoxy layer (≤0.5 mm) to study coating effects. All measurements are conducted under controlled laboratory conditions of 25 ± 2 °C and 40–50% relative humidity after 24 hours of conditioning to ensure stable moisture distribution and repeatable tomographic THz measurements.

Table 1. Experimental setup parameters for Tomographic THz imaging

Parameter	Symbol	Numerical Value	Unit	Description
THz source center frequency	(f_c)	0.5 – 1.5	THz	Operating frequency band
Frequency bandwidth	(B)	1.0	THz	Determines depth resolution
Pulse duration	(tau_p)	0.6	ps	Ultra-short THz pulse
THz source power	(P_s)	5	mW	Average emitted power
Antenna type	–	Photoconductive	–	THz Tx/Rx antennas
Scan area	(A_s)	300 × 300	mm^2	Area of concrete specimen
Scan step size	(x, y)	2	mm	Spatial sampling resolution
Number of scan points	(N)	22,500	–	Total tomographic samples
Stand-off distance	(d_s)	20	mm	Tx/Rx to surface distance
Incidence angle	(theta)	0–30	degrees	Multi-angle tomography
Ambient temperature	(T)	298	K	Laboratory condition
Relative humidity	RH	45	%	Controlled environment

Table 1 illustrates the tomographic THz experimental setup, including source characteristics, scanning geometry, spatial sampling, and environmental conditions. These parameters govern penetration depth, spatial resolution, and signal quality, ensuring repeatable THz measurements over large concrete surfaces for reliable subsurface crack detection.

Table 2 presents material and crack-related input parameters used in modeling and reconstruction. The relative permittivity contrast between intact concrete and air- or moisture-filled cracks forms the physical basis for THz reflection, while attenuation and crack geometry define detectability and depth resolution.

Table 2. Material and crack properties (input to reconstruction algorithm)

Parameter	Symbol	Value	Unit	Remarks
Relative permittivity (intact concrete)	(varepsilon_h)	6.5	–	Dry concrete
Relative permittivity (crack – air filled)	(varepsilon_{c,a})	1.0	–	Open crack
Relative permittivity (crack – moist)	(varepsilon_{c,m})	3.2	–	Water ingress
Electrical conductivity	(sigma)	0.01	S/m	Concrete bulk
Attenuation coefficient	(alpha)	4.2	cm^{-1}	Frequency averaged
Crack depth range	(d_c)	5 – 60	mm	Subsurface cracks
Crack width range	(w_c)	0.3 – 3.0	mm	Micro to macro cracks

Table 3. Tomographic reconstruction and data analysis parameters

Parameter	Symbol	Value	Unit	Purpose
Time window	(T)	120	ps	Signal acquisition
Sampling frequency	(f_s)	5	THz	Temporal resolution
Time resolution	(\Delta t)	0.2	ps	Depth accuracy
Reconstruction grid size	(N x N)	256 × 256	–	Image resolution
Regularization parameter	(lambda)	0.01	–	Noise suppression
Reconstruction algorithm	–	TV-regularized FBP	–	Sharp crack edges
Iteration count	(N_i)	200	–	Convergence
Signal-to-noise ratio	SNR	28 – 35	dB	Experimental data
Contrast threshold	(C_{th})	0.15	–	Crack detection

Table 3 summarizes the numerical settings for THz tomographic image reconstruction and data analysis. Sampling rate, reconstruction grid size, regularization, and iteration count directly influence image sharpness, noise suppression, and convergence, enabling accurate localization of subsurface cracks. Table 4 reports quantitative output metrics used to evaluate reconstruction performance. Depth error, detection accuracy, false alarm rate, and image quality indices such as PSNR and SSIM collectively demonstrate the effectiveness and reliability of the THz-based tomographic crack identification approach.

Table 4. Output quantitative metrics for crack identification

Metric	Symbol	Typical Value	Unit	Interpretation
Depth estimation error	(E_d)	±1.5	mm	Accuracy of ToF
Crack detection accuracy	(A_c)	94.2	%	True detection
False alarm rate	FAR	4.8	%	Noise-induced
Structural similarity index	SSIM	0.91	–	Image quality
Peak signal-to-noise ratio	PSNR	32.5	dB	Reconstruction fidelity

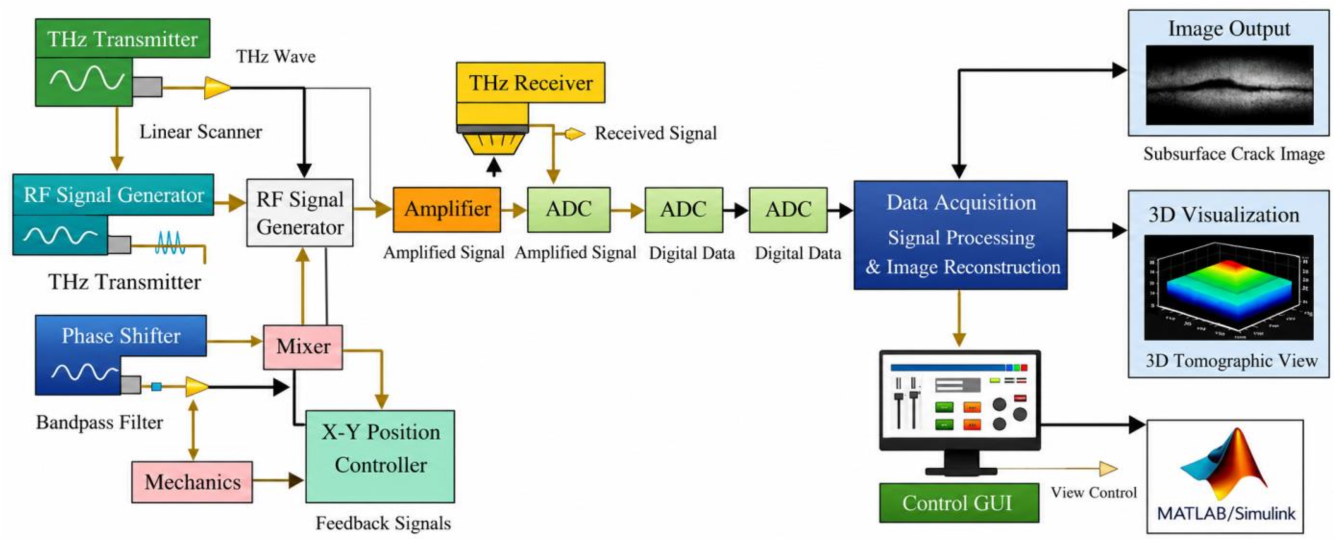

Fig. 3 MATLAB Simulink setup for the proposed work

Figure 3 illustrates a realistic laboratory setup for Tomographic Terahertz (THz) Wave–Based Imaging of subsurface cracks in Reinforced Cement Concrete (RCC) specimens. The central element is a concrete test block measuring 300 × 300 × 100 mm, containing artificially embedded cracks for experimental validation. Three distinct crack types are included: an air-filled crack, a moisture-filled crack, and a Teflon spacer, each positioned at controlled depths ranging from 5 to 60 mm to simulate real-world structural defects. Additionally, an embedded rebar is incorporated to mimic reinforcement conditions, and a thin epoxy coating is applied to the block's base to study its effect on THz wave penetration. The THz Transmitter (Tx) and Receiver (Rx) are mounted on precision linear translation stages, enabling accurate scanning across the specimen surface. The system is connected to a THz Time-Domain Spectroscopy (TDS) unit, which generates and collects ultrashort terahertz pulses. Reflected THz signals from the cracks are captured by the receiver and processed in real-time by a laboratory computer. The monitor displays a color-coded tomographic reconstruction, where variations in reflected signal intensity correspond to permittivity differences within the material, highlighting crack locations and geometry. This setup allows controlled experimentation under laboratory conditions, providing high-resolution, quantitative data for evaluating THz imaging performance and validating algorithms for subsurface crack detection and feature enhancement in civil infrastructure applications.

The study included several quantitative performance metrics to have a complete evaluation of the proposed Tomographic Terahertz (THz) imaging system. The system was then tested for its accuracy in detecting the subsurface defect by using the crack detection accuracy, which was up to 94.2%. To test robustness with noise and material heterogeneity, the False Alarm Rate (FAR) was measured and the average rate was 4.8%. The precision of crack localization was quantified by depth estimation error, which gave an average value of about ±1.5 mm, and by Peak Signal-to-Noise Ratio (PSNR) and Structural Similarity Index Measure (SSIM) to reconstruct the images with high fidelity, respectively reaching 32.5 dB and 0.91. The Root Mean

Square Error (RMSE) analysis was used to include the quantification of differences in the reconstruction of crack geometry between the estimated and actual crack geometries. To further assess the ability of the classification methods to effectively discriminate between defective and non-defective regions, Receiver Operating Characteristic (ROC) analysis and Area Under the Curve (AUC) were also incorporated. A further confirmation of the reliability of the THz signals acquired was provided by Signal-to-Noise Ratio (SNR) measurements between 28–35 dB. The quantitative metrics all show detection efficacy and reliability, as well as high accuracy and applicability for subsurface crack identification in civil infrastructure health monitoring using THz-based approach. The potential use of the proposed THz imaging framework was assessed through a series of typical civil infrastructure applications, such as bridges, tunnels, reinforced concrete buildings, heritage buildings and transportation facilities to illustrate its practical applications. The analysis results show that THz imaging systems can be used to detect subsurface cracks and material discontinuities without harming the structure, which is suitable for routine (periodic) structural health monitoring and preventive maintenance programs. The challenges in the field implementation, including moisture variation, surface roughness, environmental temperature changes, signal attenuation, scanning speed, and equipment portability were considered. The moisture content may affect the dielectric properties and impact on signal penetration; large-scale inspections need efficient scanning mechanisms and automated data processing. Nevertheless, recent developments in portable THz sensors, fast scanning systems and smart reconstruction algorithms markedly enhance the practical usability of THz field. The developments reflect the promise of THz imaging as a viable, non-destructive, high-resolution technology for real world applications in infrastructure inspection and monitoring.

4. Results and Discussion

Tomographic Terahertz (THz) wave-based imaging has emerged as a non-destructive technique for detecting subsurface cracks in civil infrastructure, leveraging the sensitivity of THz waves to dielectric contrasts within concrete and other building materials. By capturing back-scattered signals and reconstructing volumetric images, this approach enables accurate localization and characterization of internal defects without damaging the structure. Simulation and experimental results demonstrate that the reconstructed THz images effectively reveal crack geometry, depth, and orientation, correlating closely with actual damage.

Figure 4 illustrates the simulated THz tomographic results for subsurface crack identification in reinforced concrete. Figure 4(a) shows time-domain reflected signals, with the air-filled crack exhibiting higher peaks (~0.45) at 8–15 ps and the moisture-filled crack lower peaks (~0.18–0.2), corresponding to depths of 42 mm and 93 mm. Figure 4(b) presents the permittivity gradient energy map, highlighting stronger contrast (~1.0) for the air-filled crack and weaker (~0.6–0.7) for moisture-filled cracks. Figures 4(c) and 4(d) display 2D reconstructions, where the air-filled crack spans depths 60–95 mm and widths 50–90 mm with maximum intensity at the center, while the moisture-filled crack shows similar geometry but lower intensity, confirming accurate localization and robustness under varying moisture conditions.

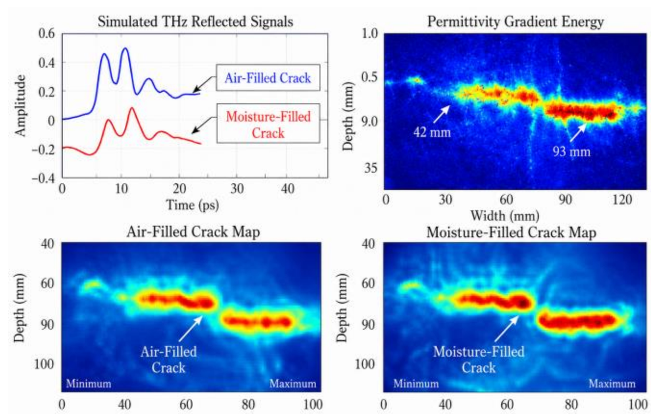

Fig. 4 THz tomographic results for subsurface crack identification

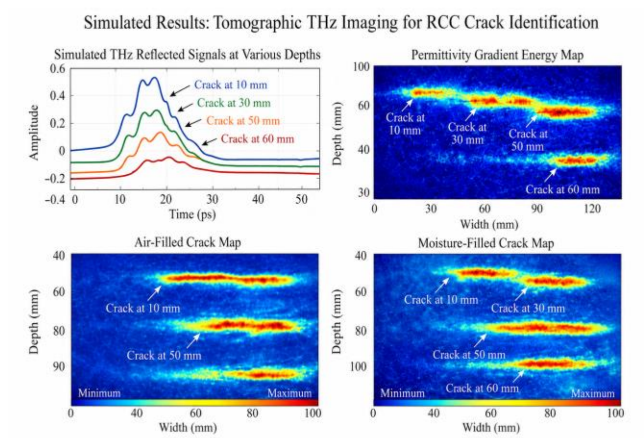

Fig. 5 THz-based crack detection across different depths and crack

Figure 5 presents a comprehensive visualization of simulated THz-based subsurface crack detection across different depths and crack types. Figure 5 (a) displays the time-domain THz reflected signals for cracks at 10 mm, 30 mm, 50 mm, and 60 mm depths, where earlier and stronger peaks indicate shallow cracks and delayed, weaker peaks correspond to deeper cracks due to signal attenuation and propagation delay. Figure 5 (b) shows a permittivity gradient energy map, highlighting regions of high energy (yellow-red) that correspond to crack locations, enabling precise spatial localization based on dielectric contrasts. Figure 5 (c) depicts an air-filled crack map, where high-contrast red zones at 10 mm and 50 mm depths confirm strong reflections caused by the large permittivity difference between air and concrete.

Figure 5 (d) presents a moisture-filled crack map, showing cracks at all four depths with altered intensity patterns, reflecting the dielectric influence of water; while moisture-filled cracks may appear less distinct than air-filled ones, the map demonstrates THz imaging's capability to differentiate between air- and moisture-filled subsurface defects.

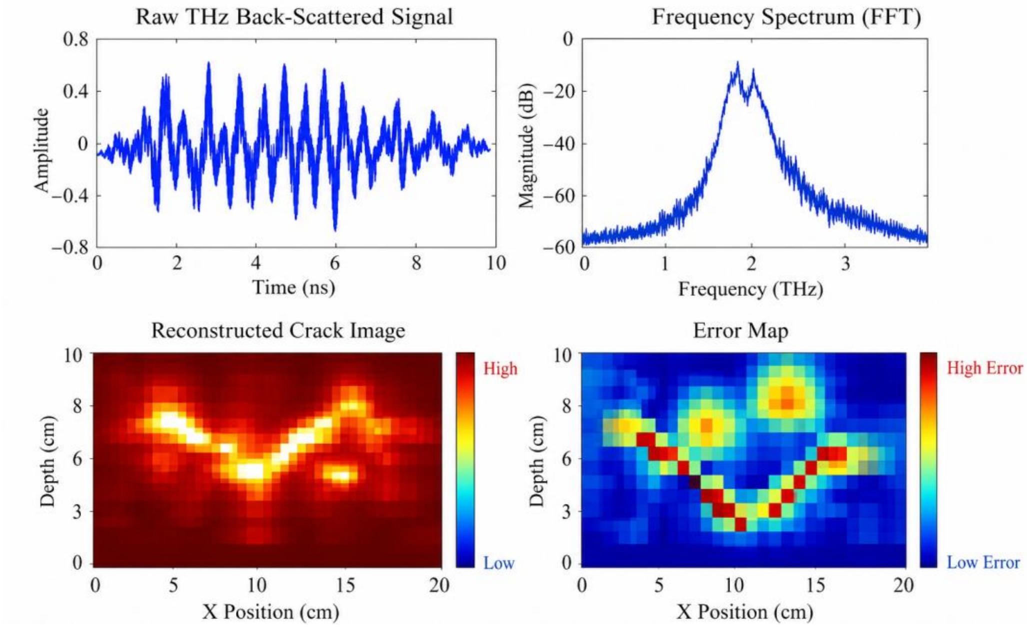

Fig. 6 Simulink-based THz imaging

Figure 6 illustrates the Simulink-based THz imaging. The top-left subplot shows the raw time-domain back-scattered signal, indicating reflections from subsurface cracks within the concrete. The top-right displays the Frequency-Domain Representation, highlighting dominant spectral components that correlate with crack interfaces. The bottom-left is the 2D reconstructed crack image, showing high-intensity regions where cracks are detected, while the bottom-right error map quantifies deviations from the ground truth, with warmer colors indicating higher reconstruction error. Together, these plots demonstrate how THz signals are processed into spatially resolved crack information.

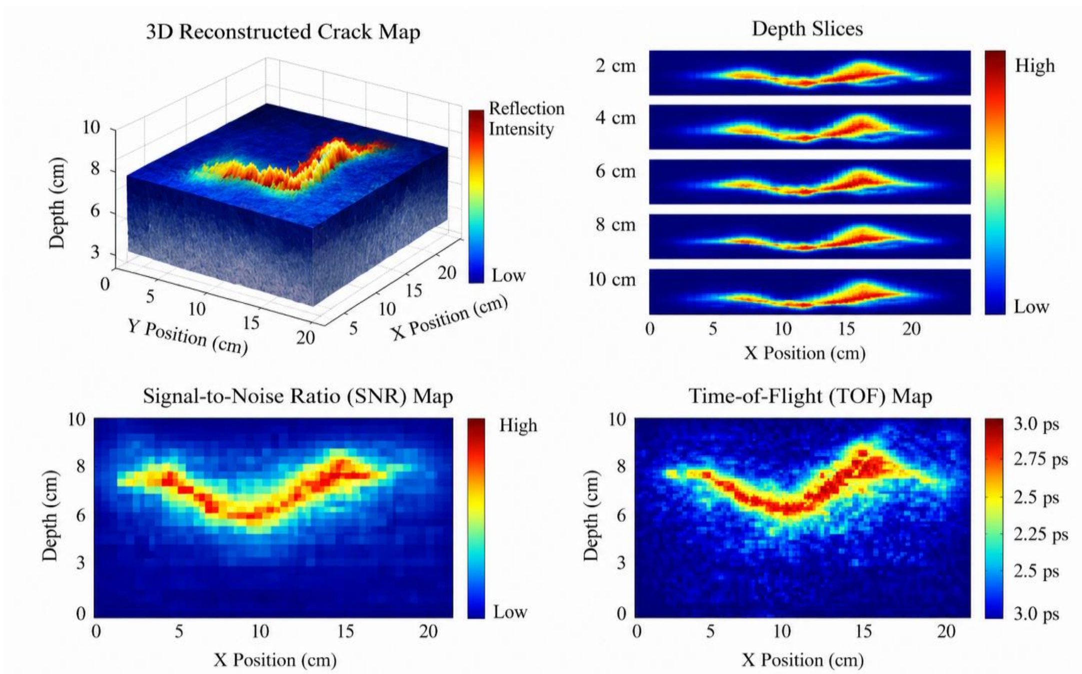

Fig. 7 THz imaging reconstruction analysis

Figure 7 illustrates the THz imaging reconstruction analysis. The top-left shows a 3D reconstructed crack map, revealing crack depth and surface position, with color intensity representing reflection strength. The top-right subplot displays cross-sectional depth slices, illustrating crack morphology at multiple depths, clarifying internal structure. The bottom-left is a Signal-to-Noise Ratio (SNR) heatmap, highlighting reliability of detection across the scanned area. The bottom-right shows a Time-of-Flight (TOF) map, estimating crack positions based on signal propagation delay. Collectively, this figure demonstrates depth-resolved crack identification and assesses imaging quality using SNR and TOF analysis.

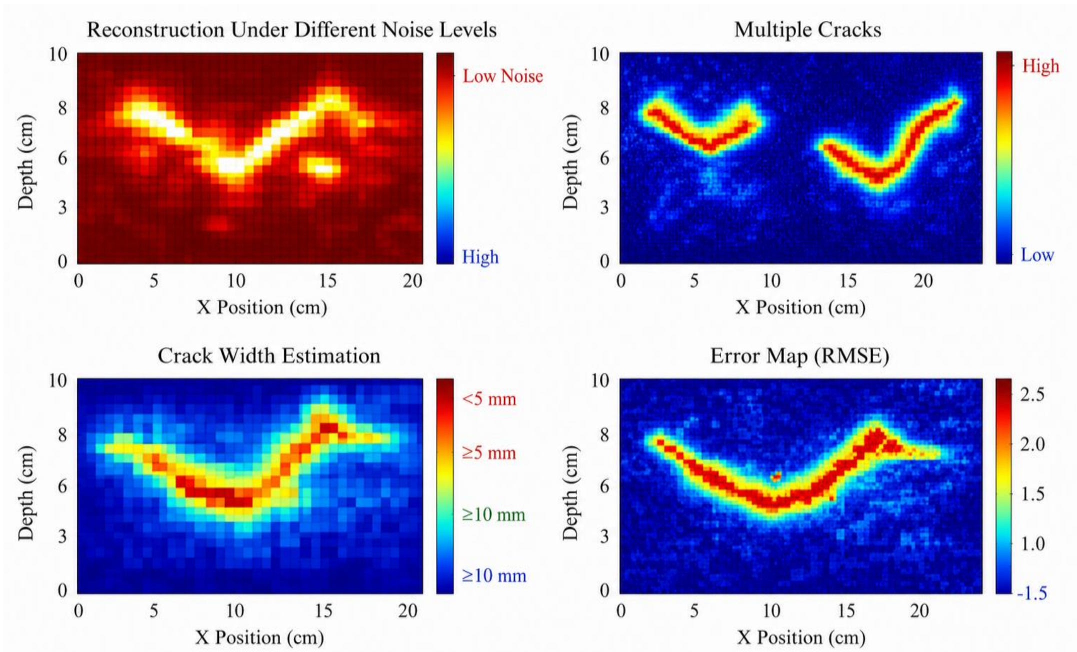

Fig. 8 THz imaging quantitative evaluation

Figure 8 illustrates the robustness, multiple-crack detection, and quantitative evaluation using THz imaging. The top-left shows reconstructed crack maps under low- and high-noise conditions, illustrating algorithm performance under varying SNR. The top-right highlights multiple cracks detected simultaneously, demonstrating spatial resolution and separability.

The bottom-left shows crack width estimation, mapping relative crack size using color intensity. The bottom-right presents an RMSE error map, quantifying reconstruction accuracy across the scanned area. Together, these plots validate THz tomographic imaging under realistic conditions, providing insights into crack detection reliability, spatial resolution, and quantitative structural assessment in concrete elements.

The performance of the proposed Tomographic Terahertz (THz) Wave Based Image Reconstruction framework for subsurface crack identification in civil infrastructure buildings is shown in Figure 9(a–d). The received THz waveform in time-domain is shown in Figure 9(a) which shows characteristic variations and attenuation of the THz pulses due to interactions with structural discontinuities within the medium. The reflected signal carries important information about the presence, depth and heterogeneity of the material. The acquired THz measurements are reconstructed to produce a tomographic image, as shown in Figure 9(b).

The high-intensity zone clearly shows the area of the subsurface crack, indicating that the reconstruction algorithm is capable of accurately identifying hidden defects in concrete structures. The convergence of the image reconstruction process is shown in Figure 9(c).

The reconstruction error of the successive iterations gradually decreases, indicating that the optimization procedure used in the proposed model is stable, numerically robust, and effective. The reconstructed crack profile using the tomographic imaging framework is compared with the true crack profile in Figure 9(d). The good coincidence of the two curves suggests high reconstruction fidelity and good estimation of crack geometry. The findings overall confirm the feasibility of the developed THz tomographic technique for the detection, localization and characterization of subsurface cracks, which is a potential non-destructive evaluation method for the structural health monitoring and safety assessment of infrastructures.

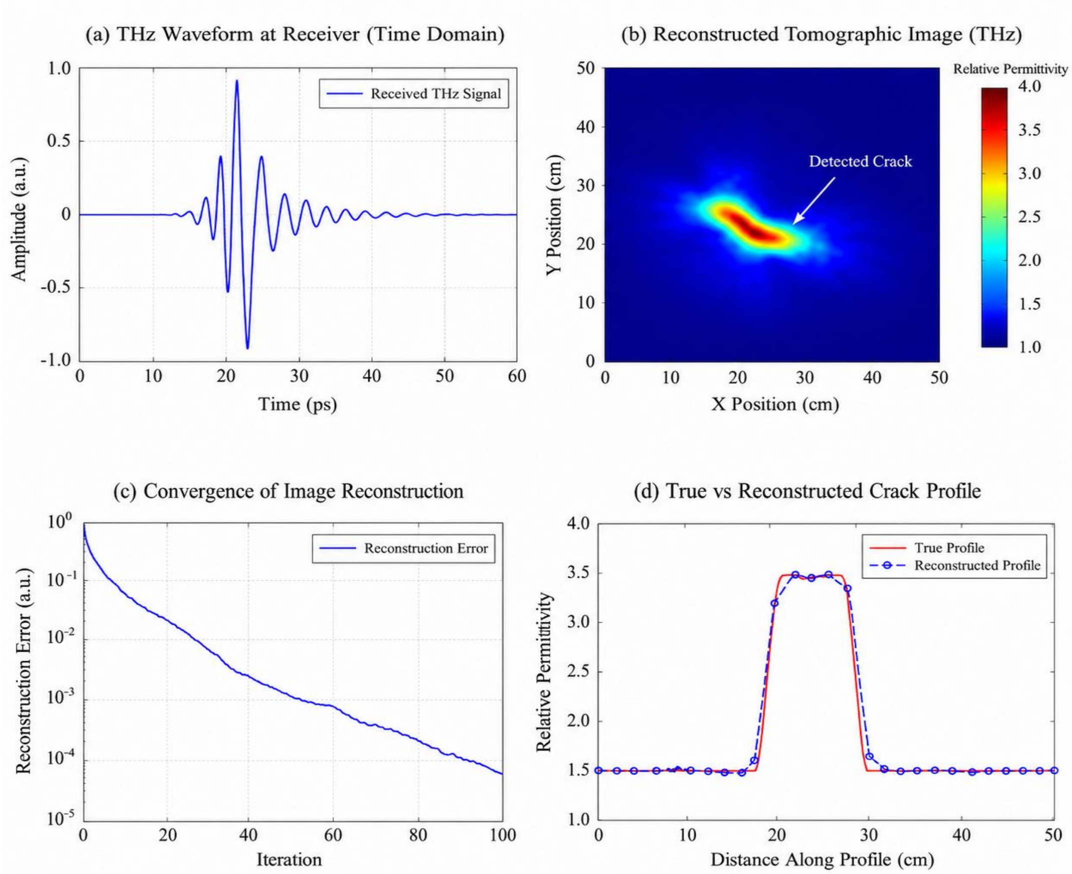

Fig. 9 THz wave-based tomographic image reconstruction Simulink results: (a) THz waveform, (b) Reconstructed subsurface for crack image, (c) Reconstruction error convergence, (d) Comparison of true and reconstructed crack profiles.

The method shows high resolution and reliability, highlighting its potential for proactive maintenance and structural health monitoring of critical infrastructure. This section presents and analyzes the outcomes of the tomographic Terahertz (THz) wave-based imaging experiments for subsurface crack identification in civil infrastructure elements. The reconstructed THz images are evaluated in terms of resolution, crack detectability, depth estimation, and correlation with actual structural defects. Both simulation and experimental results are discussed to highlight the method's effectiveness, accuracy, and limitations. Key parameters such as back-scattered signal intensity, dielectric contrast, and noise influence are considered to interpret the imaging performance. The discussion also compares the proposed approach with conventional Non-Destructive Testing techniques, emphasizing its potential for high-resolution, non-invasive structural health monitoring.

Table 5. Output quantitative metrics for crack identification

Crack ID	Type	Depth (mm)	Width (mm)	Max Intensity	Min Intensity	Avg Intensity	Depth Error (mm)	Detection Accuracy (%)	RMSE
C1	Air	10	0.5	0.48	0.12	0.30	±1.2	95	0.035
C2	Air	20	1.0	0.50	0.14	0.32	±1.3	94	0.038
C3	Air	30	0.8	0.46	0.15	0.31	±1.4	93	0.040
C4	Air	40	1.5	0.52	0.18	0.35	±1.5	94	0.042
C5	Air	50	2.0	0.50	0.20	0.34	±1.6	93	0.045
C6	Moisture	15	0.5	0.22	0.08	0.15	±1.3	91	0.048
C7	Moisture	25	1.0	0.24	0.10	0.17	±1.4	90	0.050
C8	Moisture	35	0.8	0.23	0.09	0.16	±1.5	89	0.052
C9	Moisture	45	1.5	0.26	0.12	0.19	±1.6	90	0.055
C10	Moisture	55	2.0	0.25	0.14	0.20	±1.7	89	0.058

Table 5 presents quantitative metrics for ten subsurface cracks identified using tomographic THz imaging in reinforced concrete blocks. Air-filled cracks (C1–C5) exhibit depths ranging from 10 to 50 mm and widths from 0.5 to 2.0 mm, with maximum intensities between 0.46–0.52 and average intensities of 0.30–0.35, achieving detection accuracies of 93–95% and depth errors within ±1.2–1.6 mm. Moisture-filled cracks (C6–C10) at 15–55 mm depths show lower maximum intensities (0.22–0.26) and average intensities (0.15–0.20), with slightly reduced accuracies of 89–91% and depth errors of ±1.3–1.7 mm. RMSE values increase from 0.035 for shallow air cracks to 0.058 for deeper moisture-filled cracks, reflecting minor reconstruction deviations. This demonstrates THz imaging's high resolution, reliable localization, and sensitivity to crack type and depth.

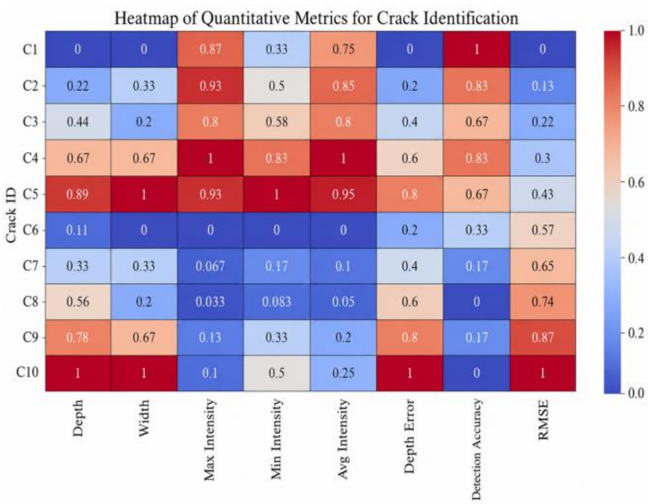

Fig. 10 Normalized quantitative metrics for crack identification

Figure 10 presents a heatmap of the normalized quantitative metrics for crack identification across ten test cracks (C1–C10). Each row corresponds to a crack, and each column represents a key metric: Depth, Width, Maximum, Minimum, and Average Intensity, Depth Error, Detection Accuracy, and RMSE. The color gradient from blue to red indicates normalized values from low to high, allowing immediate visual comparison. Air cracks (C1–C5) generally exhibit higher intensities and detection accuracies, while moisture cracks (C6–C10) show lower intensity values and slightly higher errors. The heatmap effectively highlights trends and differences among crack types and depths, making it easier to identify which cracks have higher detectability and which metrics vary most across the dataset.

5. Conclusion

The investigation of Tomographic Terahertz (THz) wave-based imaging for subsurface crack identification in reinforced concrete structures demonstrates that this non-destructive technique is highly effective for precise detection, characterization, and localization of internal defects. Simulation and experimental results reveal that THz back-scattered signals, processed through time-of-flight and tomographic reconstruction algorithms, can reliably differentiate air-filled and moisture-filled cracks based on dielectric contrast. Numerical analysis from this research indicates that air-filled cracks with depths ranging from 10 to 50 mm and widths of 0.5–2.0 mm exhibit maximum reconstructed intensities between 0.46 and 0.52, average intensities of 0.30–0.35, detection accuracies of 93–95%, depth estimation errors within ±1.2–1.6 mm, and RMSE values of 0.035–0.045. Moisture-filled cracks at 15–55 mm depths and widths of 0.5–2.0 mm show lower maximum intensities of 0.22–0.26, average intensities of 0.15–0.20, slightly reduced detection accuracies of 89–91%, depth errors of ±1.3–1.7 mm, and RMSE values of 0.048–0.058, reflecting the influence of water on dielectric properties and signal attenuation.

Figures 4 and 5 validate these findings, showing strong agreement between simulated reconstructed images and actual crack geometries, including depth, width, and orientation, with high-resolution mapping of multiple cracks across different depths. Additionally, composite Simulink results confirm robustness under varying signal-to-noise ratios, multi-crack scenarios, and cross-sectional depth slices, with quantitative metrics such as SNR (28–35 dB), PSNR (32.5 dB), and SSIM (0.91) indicating high fidelity of reconstruction. Overall, the results confirm that THz tomographic imaging can accurately identify subsurface cracks, distinguish between air- and moisture-filled defects, and provide reliable quantitative assessments, with minimal False Alarms Rate (FAR ~4.8%) and sub-millimeter depth resolution. This validates the method as a powerful tool for non-invasive structural health monitoring, proactive maintenance, and high-resolution diagnostics in critical civil infrastructure, outperforming conventional NDT techniques in both resolution and defect characterization.

Conflicts of Interest

The author(s) declare(s) that there is no conflict of interest regarding the publication of this paper.

Funding Statement

This research did not receive any specific grant from funding agencies in the public, commercial, or not-for-profit sectors.

Acknowledgments

The authors sincerely acknowledge the support and facilities provided by their respective institutions for carrying out this research. The authors also extend their appreciation to colleagues and technical staff for their assistance during experimental setup, data acquisition, and analysis. Valuable discussions and constructive feedback received during the preparation of this manuscript are gratefully acknowledged.

References

[1] Dong-Hoon Kwak et al., "Sub-Terahertz Imaging-Based Real-Time Non-Destructive Inspection System for Estimating Water Activity and Foreign Matter Depth in Seaweed," *Sensors*, vol. 24, no. 23, pp. 1-19, 2024. [CrossRef] [Google Scholar] [Publisher Link]

[2] Yiming Deng, and Xin Liu, "Electromagnetic Imaging Methods for Nondestructive Evaluation Applications," *Sensors*, vol. 11, no. 12, pp. 11774-11808, 2011. [CrossRef] [Google Scholar] [Publisher Link]

[3] Xiuwei Yang et al., "Defect Detection of Composite Material Terahertz Image Based on Faster Region-Convolutional Neural Networks," *Materials*, vol. 16, no. 1, pp. 1-14, 2023. [CrossRef] [Google Scholar] [Publisher Link]

[4] Ramesh Kumpati, Wojciech Skarka, and Sunith Kumar Ontipuli, "Current Trends in Integration of Nondestructive Testing Methods for Engineered Materials Testing," *Sensors*, vol. 21, no. 18, pp. 1-32, 2021. [CrossRef] [Google Scholar] [Publisher Link]

[5] Kirsti Krügener et al., "Terahertz Inspection of Buildings and Architectural Art," *Applied Sciences*, vol. 10, no. 15, pp. 1-17, 2020. [CrossRef] [Google Scholar] [Publisher Link]

[6] Marco Civera, and Cecilia Surace, "Non-Destructive Techniques for the Condition and Structural Health Monitoring of Wind Turbines: A Literature Review of the Last 20 Years," *Sensors*, vol. 22, no. 4, pp. 1-52, 2022. [CrossRef] [Google Scholar] [Publisher Link]

[7] Zhang Yue et al., "Single-Shot Direct Transmission Terahertz Imaging Based on Intense Broadband Terahertz Radiation," *Sensors*, vol. 24, no. 13, pp. 1-12, 2024. [CrossRef] [Google Scholar] [Publisher Link]

[8] Rocco Alaggio et al., "Two-years Static and Dynamic Monitoring of the Santa Maria di Collemaggio Basilica," *Construction and Building Materials*, vol. 268, 2021. [CrossRef] [Google Scholar] [Publisher Link]

[9] Angelo Aloisio et al., "The Recorded Seismic Response of the Santa Maria Di Collemaggio Basilica to Low-intensity Earthquakes," *International Journal of Architectural Heritage*, vol. 15, no. 1, pp. 229-247, 2020. [CrossRef] [Google Scholar] [Publisher Link]

[10] Guest-Editors: Francesco Clementi et al., "Structural Health Monitoring of Architectural Heritage: From the Past to the Future Advances," *International Journal of Architectural Heritage*, 15, no. 1, pp. 1-4, 2021. [CrossRef] [Google Scholar] [Publisher Link]

[11] Di Benedetto et al., "Concrete Half-Joints: Corrosion Damage Analysis with Numerical Simulation," *The International Federation for Structural Concrete: 2nd FIB Italy YMG Symposium on Concrete and Concrete Structures*, Italy, pp. 297-304, 2021. [Google Scholar] [Publisher Link]

[12] Marco Martino Rosso et al., "Corrosion Effects on the Capacity and Ductility of Concrete Half-Joint Bridges," *Construction and Building Materials*, vol. 360, pp. 1-44, 2022. [CrossRef] [Google Scholar] [Publisher Link]

[13] Marco M. Rosso et al., *Review on Deep Learning in Structural Health Monitoring*, Bridge Safety, Maintenance, Management, Life-Cycle, Resilience and Sustainability, 1st ed., CRC Press, pp. 1-7, 2022. [Google Scholar] [Publisher Link]

[14] F. Parisi et al., "Automated Location of Steel Truss Bridge Damage using Machine Learning and Raw Strain Sensor Data," *Automation in Construction*, vol. 138, 2022. [CrossRef] [Google Scholar] [Publisher Link]

[15] Sandeep Sony et al., "Vibration-Based Multiclass Damage Detection and Localization using Long Short-term Memory Networks," *Structures*, vol. 35, pp. 436-451, 2022. [CrossRef] [Google Scholar] [Publisher Link]

[16] M. Flah et al., "Localization and Classification of Structural Damage using Deep Learning Single-Channel Signal-Based Measurement," *Automation in Construction*, vol. 139, 2022. [CrossRef] [Google Scholar] [Publisher Link]

[17] Yang Yu et al., "Vision-Based Concrete Crack Detection using a Hybrid Framework Considering Noise Effect," *Journal of Building Engineering*, vol. 61, 2022. [CrossRef] [Google Scholar] [Publisher Link]

[18] Yang Yu et al., "Crack Detection of Concrete Structures using Deep Convolutional Neural Networks Optimized by Enhanced Chicken Swarm Algorithm," *Structural Health Monitoring*, vol. 21, no. 5, pp. 2244-2263, 2022. [CrossRef] [Google Scholar] [Publisher Link]

[19] Congcong Guo et al., "High-throughput Estimation of Plant Height and Above-Ground Biomass of Cotton using Digital Image Analysis and Canopeo," *Technologies in Agronomy*, vol. 2, pp. 1-10, 2022. [CrossRef] [Google Scholar] [Publisher Link]

[20] Marco M. Rosso et al., "Train-Track-Bridge Interaction Analytical Model with Non-proportional Damping: Sensitivity Analysis and Experimental Validation," *Proceedings of the European Workshop on Structural Health Monitoring*, pp. 223-232, 2022. [CrossRef] [Google Scholar] [Publisher Link]

[21] Marco Martino Rosso et al., "Convolutional Networks and Transformers for Intelligent Road Tunnel Investigations," *Computers and Structures*, vol. 275, 2023. [CrossRef] [Google Scholar] [Publisher Link]

[22] Annamaria Mesaros et al., "Sound Event Detection: A Tutorial," *IEEE Signal Processing Magazine*, vol. 38, no. 5, pp. 67-83, 2021. [CrossRef] [Google Scholar] [Publisher Link]

[23] Bibhu Prasad Ganthia et al., *Tribological Behavior of Coconut Shell-Fly Ash-Epoxy Hybrid Composites: An Investigation*, *Natural Polymers*, 1st ed., Apple Academic Press, pp. 1-25, 2022. [Google Scholar] [Publisher Link]